



Journal Website:  
<http://sciencebring.com/index.php/ijasr>

Copyright: Original content from this work may be used under the terms of the creative commons attributes 4.0 licence.

 Research Article

## Study of The Thermodynamics of The Propane-Butane Fraction Pyrolysis Process

**Submission Date:** March 13, 2025, **Accepted Date:** April 09, 2025,

**Published Date:** May 11, 2025

**Crossref doi:** <https://doi.org/10.37547/ijasr-05-05-03>

### Normurot I. Fayzullayev

Doctor of Chemical Sciences, Professor, Samarkand State University named after Sharof Rashidov, Institute of Biochemistry, Department of Polymer Chemistry and Chemical Technologies, Samarkand, Uzbekistan

### Sanjar H. Saidqulov

Laboratory assistant, Department of Polymer Chemistry and Chemical Technologies, Institute of Biochemistry, Samarkand State University named after Sharof Rashidov, Samarkand, Uzbekistan

### Khamdam I. Akbarov

Doctor of Chemical Sciences, Professor, National University of Uzbekistan, Department of Physical Chemistry, Tashkent, Uzbekistan

### Hayitali N. Ibodullayev

Student, Institute of Biochemistry, Samarkand State University named after Sharof Rashidov, Samarkand, Uzbekistan

## ABSTRACT

This study focuses on enhancing the sorption and catalytic properties of high-silica mesoporous zeolites (HSMZs) and investigating the pyrolysis processes of the propane-butane fraction at elevated temperatures. The HSMZ samples were decationized using a 25% ammonium chloride solution and modified to their H-form aluminosilicate states. Various metal oxides such as CuO, Li<sub>2</sub>O, La<sub>2</sub>O<sub>3</sub>, ZnO, Fe<sub>2</sub>O<sub>3</sub>, and BaO were employed as modifiers in different concentrations. Using the modified zeolites, the thermal and catalytic pyrolysis of propane-butane hydrocarbon mixtures was carried out in a flow reactor at high temperatures (~650–800 °C). To evaluate catalytic activity, a comparative analysis was conducted between thermal and catalytic cracking results. The selectivity and overall yields of unsaturated C<sub>2</sub>–C<sub>4</sub> hydrocarbons, including ethylene and propylene, were measured. The catalysts were prepared via extrusion and tableting methods, and their structures were characterised using infrared spectroscopy (IR)

and X-ray phase analysis. The IR spectra revealed absorption bands at 1120, 800, 560, and 460  $\text{cm}^{-1}$ , indicating the crystallinity and framework structure of the HSMZs. Thermodynamic calculations of dehydrogenation, cracking, and dehydrocracking of low-molecular-weight saturated hydrocarbons (propane and butane) were performed in the range of 200–800 °C. Based on the changes in Gibbs free energy ( $\Delta G^0$ ) and equilibrium constants ( $K^0$ ), the temperature-dependent stability of each process was assessed. The results allowed for the identification of optimal temperature intervals for obtaining valuable unsaturated hydrocarbons from propane-butane mixtures. These findings provide insights for modelling high-temperature thermal and catalytic processes, improving the use of modified zeolites, and increasing the selectivity of the resulting products.

**Objective:** To study the thermodynamics of the propane-butane fraction pyrolysis process.

## KEYWORDS

Propane-butane fraction, flow and pulse modes, high-temperature thermal process, propylene, HSMZ, IR spectra.

## INTRODUCTION

The pyrolysis of hydrocarbons at elevated temperatures in the absence of oxygen is a widely studied process; however, comparative experimental data concerning this process under continuous flow conditions remain scarce in the literature. Particularly, there is a lack of systematic investigations that allow for the comparison of results obtained under different flow regimes and temperature intervals during the thermal cracking of propane-butane hydrocarbon mixtures. To ensure consistent conversion levels, experimental conditions must be designed such that the reaction proceeds in the kinetic domain and the molecular structure of the saturated hydrocarbons remains relatively unaltered at the onset of decomposition.

Under pulse reaction systems, it becomes feasible to observe the “quasi-stationary” state of the catalyst, in which the composition of the resulting

products becomes independent of the number of pulses applied. This approach allows for detailed analysis of the catalytic behaviour and product distribution during the pyrolysis of propane-butane mixtures at high temperatures in an inert environment [1–3].

Nevertheless, the thermal pyrolysis of propane and butane often leads to increased coke formation and high energy consumption, posing significant technological challenges. Currently, there are no industrial-scale processes available for the high-temperature, oxygen-free catalytic conversion of  $\text{C}_3$ – $\text{C}_4$  saturated hydrocarbons into valuable light olefins such as ethylene and propylene. Despite the existence of several mechanistic models describing the conversion of such hydrocarbons over high-silica mesoporous zeolites (HSMZs), these models typically focus on generalised product formation pathways and often lack selectivity control [4–8].

Moreover, only a limited number of catalysts with high catalytic activity and selectivity have been developed for these transformations. High-silica mesoporous zeolites, particularly aluminosilicates, offer promising structural and acidic properties for such catalytic processes. However, the characteristics and behaviour of various metal oxide modifiers introduced into these zeolites to enhance their performance remain insufficiently studied.

Therefore, a comprehensive understanding of the relationship between the acidic and catalytic properties of modified HSMZs and their performance in the conversion of C<sub>3</sub>-C<sub>4</sub> hydrocarbons is essential for the development of efficient and selective catalysts for industrial applications [9-15].

## METHODS

In order to enhance the sorption and catalytic performance of high-silica mesoporous zeolites (HSMZs), a decationization process was carried out using a 25% aqueous solution of ammonium chloride. Specifically, 10 g of HSMZ aluminosilicate

was added to 100 mL of the ammonium chloride solution. The mixture was stirred mechanically and maintained in a water bath at 90 °C for 4 hours to ensure uniform treatment and effective ion exchange. After completion, the treated zeolite was filtered through a Büchner funnel to separate the solid phase, then washed thoroughly with distilled water to remove residual ions and dried under ambient conditions. Finally, the dried sample was calcined in a muffle furnace at 550 °C for 5 hours to activate the acidic sites and stabilise the framework structure.

The crystalline structure of the zeolites was characterised using X-ray diffraction (XRD), performed on a DRON-4 diffractometer equipped with a molybdenum anode and a nickel filter. The diffraction patterns were analysed to determine interplanar spacings (d-values) and peak intensities. The observed diffraction lines (peak positions and relative intensities) were interpreted by comparison with standard reference samples of highly crystalline HSMZs, which were known to be free of amorphous phases, as confirmed by Fourier-transform infrared (FTIR) spectroscopy.

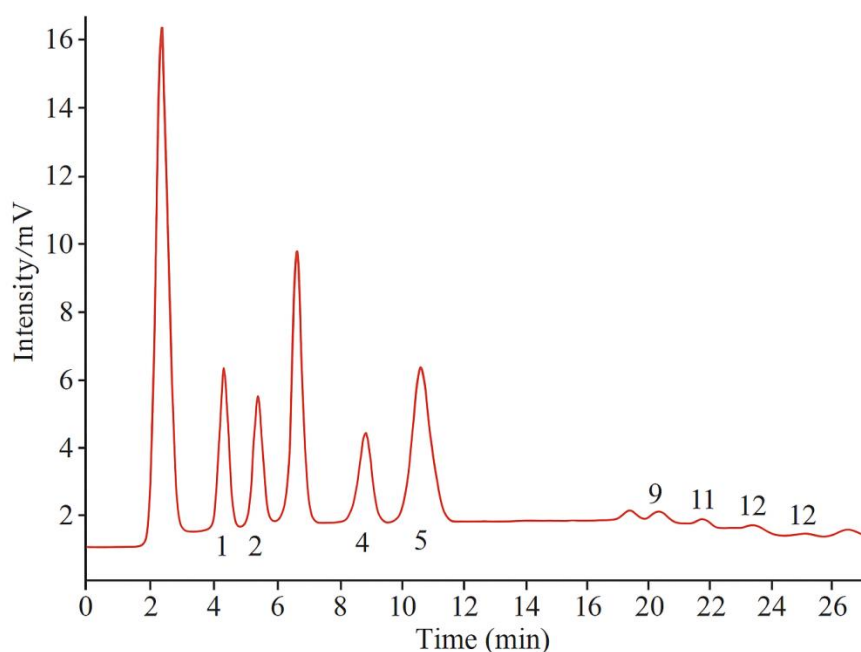


**Figure 2. Chromatogram of the liquid products formed during the conversion of low-molecular-weight saturated hydrocarbons ( $C_3$ – $C_4$  fraction), showing the following compounds: 1 – Benzene, 2 – Toluene, 3 – m,p-Xylene, 4 – o-Xylene, 5 – Mesitylene, 6 – Pseudocumene, 7 – m-Diethylbenzene, 8 – p-Diethylbenzene, 9 – 1,2-Dimethyl-3-ethylbenzene, 10 – Naphthalene, 11 –  $\alpha$ -Methylnaphthalene, 12 –  $\beta$ -Methylnaphthalene.**

The chromatographic analysis of the liquid-phase pyrolysis products was performed to identify the aromatic and alkylaromatic compounds formed during the catalytic conversion of the  $C_3$ – $C_4$  hydrocarbon fraction. The chromatogram (Figure 2) revealed the presence of several key compounds including: 1 – Benzene, 2 – Toluene, 3 – m,p-Xylene, 4 – o-Xylene, 5 – Mesitylene, 6 – Pseudocumene, 7 – m-Diethylbenzene, 8 – p-Diethylbenzene, 9 – 1,2-Dimethyl-3-ethylbenzene, 10 – Naphthalene, 11 –  $\alpha$ -Methylnaphthalene, 12 –  $\beta$ -Methylnaphthalene.

These results were used for further analysis of selectivity, reaction pathways, and the catalytic influence of modified HSMZs.

## RESULTS AND DISCUSSION

Modification of High-Silica Mesoporous Zeolites with Enhanced Sorption and Catalytic Properties

The modification of high-silica mesoporous zeolites (HSMZs) exhibiting superior sorption and catalytic characteristics was carried out by impregnating the H-form aluminosilicate samples (H-HSMZ) with aqueous solutions of selected metal salts. The concentration of the metal salt solutions was calculated according to the moisture capacity of the zeolite sample to match the desired content of the metal or metal oxide. The impregnation process involved continuous stirring in a water

bath at 90 °C until the complete evaporation of moisture. Subsequently, the samples were dried at 110 °C for 8 hours and calcined in a muffle furnace at 550 °C for 4 hours in air.

As a result, a series of modified HSMZ catalysts were prepared with the following compositions:

- 2% CuO/H-HSMZ
- 1%, 2%, or 3% Li<sub>2</sub>O/H-HSMZ
- 2% La<sub>2</sub>O<sub>3</sub>/H-HSMZ
- 2% K<sub>2</sub>O-ZnO/H-HSMZ
- 2% K<sub>2</sub>O-Fe<sub>2</sub>O<sub>3</sub>/H-HSMZ

- 2% Li<sub>2</sub>O-BaO/H-HSMZ

These modified zeolites were used as catalysts for the high-temperature pyrolysis of propane-butane hydrocarbon mixtures under oxygen-free conditions. The goal was to determine their catalytic performance in comparison with purely thermal decomposition under identical experimental conditions.

Table 1 presents the typical results of catalytic and thermal pyrolysis of propane-butane mixtures (~50% conversion) in a continuous flow regime under oxygen-free high-temperature conditions.

**Table 1. Comparison of Catalytic and Thermal Pyrolysis of Propane-Butane Hydrocarbon Mixtures at High Temperatures in Flow Regime (~50% Conversion)**

Days	T, °C	T, °C	Propane-butane hydrocarbon mixture conversion, %	Productivity in relation to transferred raw materials, mass %					Selectivity on C <sub>2</sub> H <sub>4</sub> , %
				CH <sub>4</sub>	C <sub>2</sub> H <sub>6</sub>	C <sub>2</sub> H <sub>4</sub>	C <sub>3</sub> H <sub>6</sub>	ΣC <sub>2</sub> -C <sub>4</sub> molecularly unsaturated ethylene series hydrocarbons	
1		655	14.8	2.7	1.0	3.4	7.7	11.1	23.0
		680	17.6	3.8	1.0	5.7	7.1	12.8	32.4
		735	84.4	28.0	8.4	31.8	16.2	48.0	37.7
		750	95.0	40.4	9.7	38.6	6.3	44.9	40.6
		655	14.6	2.4	1.0	2.6	8.6	11.2	17.8
2		680	35.7	8.9	3.9	9.7	13.2	22.9	27.2
		725	83.4	31.2	9.0	29.6	13.6	43.2	35.5
		750	95.0	37.4	9.8	37.3	10.5	47.8	39.3
		665	46.6	10.7	4.4	12.1	19.4	31.5	26.0
		685	72.3	20.1	6.2	25.8	20.2	46.0	35.7
3		720	90.0	26.6	9.8	33.2	20.4	53.6	36.9

	755	94.9	39.9	10.2	40.4	4.4	44.8	42.6
	755	86.3	21.8	6.8	32.6	25.1	57.7	37.8
	770	93.4	31.8	7.7	40.7	13.2	53.9	43.6
	780	97.0	34.5	6.0	47.5	9.0	56.5	49.0

### Structural and Spectroscopic Analysis of High-Silica Mesoporous Zeolite Catalysts

It was found that the thermal decomposition of saturated hydrocarbons in a high-temperature, oxygen-free environment under flow conditions is almost identical to that observed in static batch setups. This similarity enables rapid kinetic studies of catalytic processes across multiple systems within a short time frame.

For catalytic testing, optimal zeolite-based catalyst fractions were prepared using extrusion and tablet pressing techniques. Two methods were employed to shape the high-silica zeolite samples:

- **Method 1 (Pressing):** Zeolite powders were compressed into tablets with a diameter of 16 mm and a thickness of 2–3 mm under 250 kg/cm<sup>2</sup> pressure using a steel mould. These tablets were crushed and sieved to obtain particle fractions in the 1.5–2.0 mm<sup>2</sup> range using metal mesh sieves.

- **Method 2 (Extrusion):** Zeolite powders were mixed with a binder (pseudoboehmite), diluted nitric acid or ammonia solution, and distilled water until a viscous paste was obtained. The mass was extruded through a mould and cut to the desired size. It was dried at 110 °C for 12 hours, then calcined at 550 °C for 4 hours. The desired fraction (1.5–2.0 mm<sup>2</sup>) was separated by sieving.

The structure of the resulting aluminosilicate-based zeolite catalysts was analysed using infrared (IR) spectroscopy in the mid-IR region (400–2000 cm<sup>-1</sup>), which includes characteristic absorption bands associated with the vibrational modes of AlO<sub>4</sub><sup>2-</sup> and SiO<sub>4</sub><sup>2-</sup> crystal tetrahedra.

To prepare samples for IR analysis, 1–2 mg of the zeolite was mixed with 400 mg of KBr, pressed into a ring mould, and placed into the spectrometer. The observed absorption bands (ABs) arise from two types of vibrational modes:

1. **Primary internal vibrations** within the TO<sub>4</sub> tetrahedra, which form the structural units of the aluminosilicate framework. These do not reflect changes in the external structure.
2. **External vibrations** along the linkages between tetrahedra. These are more sensitive to the zeolite's topology, secondary building units, and pore structure.

The following major absorption bands were observed:

- **1120 cm<sup>-1</sup>** – intense band attributed to antisymmetric stretching of TO<sub>4</sub> tetrahedra.
- **800 cm<sup>-1</sup>** – indicative of symmetric stretching vibrations, primarily involving SiO<sub>4</sub> units.

- **560 cm<sup>-1</sup>** – bending vibrations sensitive to the topology and connectivity of secondary structural units (e.g., 5-membered or 6-membered rings).
- **460 cm<sup>-1</sup>** – bending vibrations within TO<sub>4</sub> tetrahedra.

The presence of these bands confirms the structural classification of all tested samples within the HSMZ family. The intensity ratio of the absorption bands at 560 cm<sup>-1</sup> and 460 cm<sup>-1</sup> ( $\log I_{560}/\log I_{460} \times 100$ ) was used to calculate the degree of crystallinity for each sample. The calculated crystallinity values for different SiO<sub>2</sub>/Al<sub>2</sub>O<sub>3</sub> ratios were as follows:

**Table 2. Crystallinity Degree of Modified High-Silica Mesoporous Zeolites Based on SiO<sub>2</sub>/Al<sub>2</sub>O<sub>3</sub> Molar Ratio**

No.	Sample Description	SiO <sub>2</sub> /Al <sub>2</sub> O <sub>3</sub> Ratio	Crystallinity (%)
1	Modified HSMZ Catalyst	27	83
2	Modified HSMZ Catalyst	33	81
3	Modified HSMZ Catalyst	49	94
4	Modified HSMZ Catalyst	67	85
5	Modified HSMZ Catalyst	90	93
6	Modified HSMZ Catalyst	125	78
7	Ferro-silicate-based Catalyst Sample	–	85

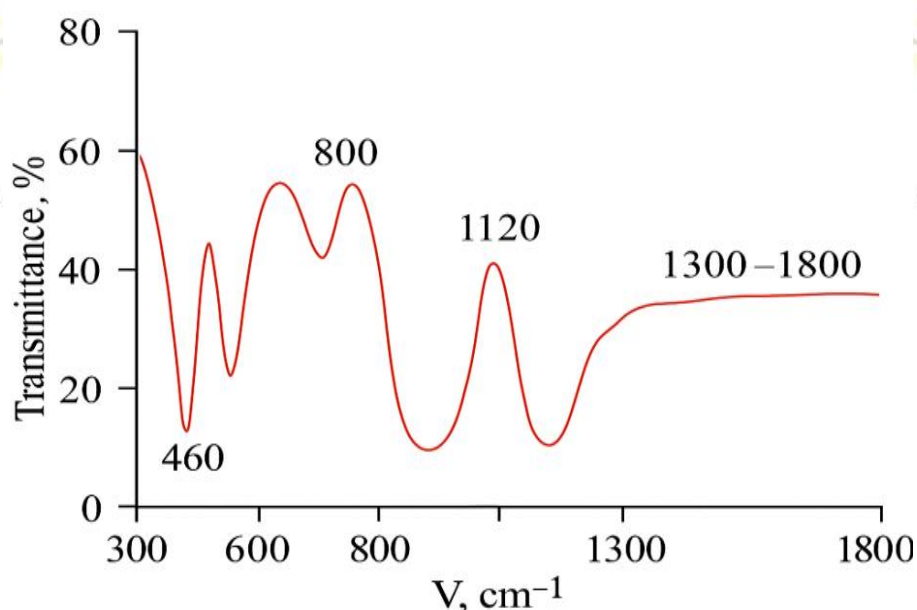


**Figure 2. IR Spectrum of Decationized H-HSMZ-70 Sample**  
Y-axis: Transmittance (%); X-axis: Wavenumber (cm<sup>-1</sup>)

## Thermodynamic Aspects of the Transformation of Light Hydrocarbons

Saturated hydrocarbons are thermally stable compounds and decompose only at high temperatures. The ultimate products of complete thermal decomposition are carbon and hydrogen. The thermal stability of a hydrocarbon can be evaluated using the change in its Gibbs free energy of formation:

$$\Delta G^0 = \Delta H^0 - T\Delta S^0 \quad (1)$$

This value is also related to the equilibrium constant  $K_p$  through the expression:

$$-\Delta G^0 = RT \ln K_p \quad (2)$$

At temperatures up to 560 °C, the most thermodynamically stable light hydrocarbon is methane (as shown in Figures 3-5). At temperatures exceeding 560 °C, the most probable thermodynamic system shifts toward a mixture of elemental carbon and hydrogen. As temperature increases, the standard Gibbs free energy change ( $\Delta G^0$ ) for all hydrocarbons (except acetylene) increases, indicating a decrease in their thermal stability.

In contrast, the thermal stability of unsaturated hydrocarbons (such as ethylene and its homologues) decreases more gradually with rising temperature compared to saturated hydrocarbons of similar molecular weight. For instance, ethylene remains more thermodynamically stable than saturated hydrocarbons with the same number of carbon atoms — such as butene and propylene —

at temperatures above 805 °C, whereas butenes and propylene lose stability around 650–670 °C.

This difference in thermal stability explains why unsaturated hydrocarbons of the ethylene series can be obtained through thermal transformations of saturated hydrocarbons under high-temperature conditions. The feasibility of such transformations is rooted in the thermodynamic disparity between these molecular species.

In addition to decomposition into elements, the conversion of propane–butane fractions may proceed via several other thermodynamically feasible pathways, including:

- Dehydrogenation,
- C–C bond cleavage, and
- Dehydrocracking (combined dehydrogenation and carbon–carbon bond breaking).

For example:

- C–C bond cleavage in propane becomes thermodynamically favourable above 350 °C.
- Butane conversion to methane and propylene occurs above 320 °C,
- Butane to ethane and ethylene becomes favourable above 420 °C,
- Dehydrocracking of butane becomes feasible at temperatures exceeding 610 °C.

The temperature dependence of the logarithmic equilibrium constant  $\log K_p$  for these reactions was

calculated using Equation (2) and is illustrated in Figure 6.

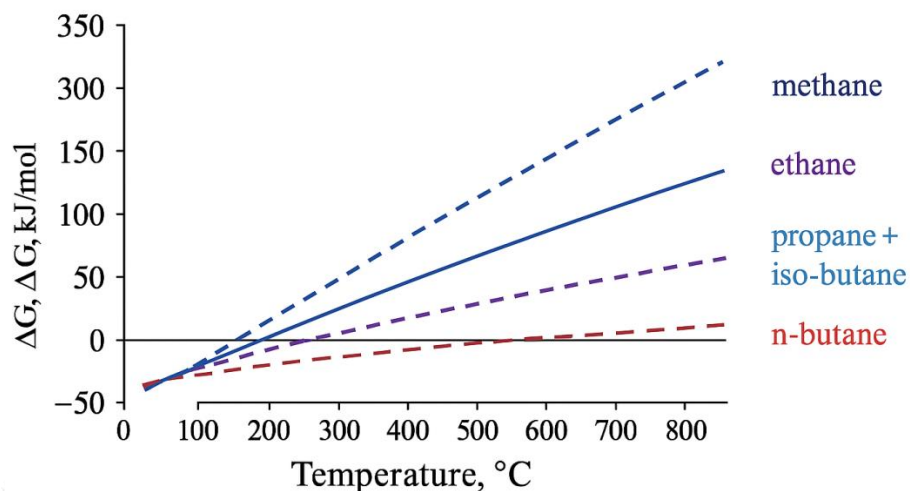


Figure 3. Effect of temperature on the thermodynamic stability of saturated hydrocarbons.

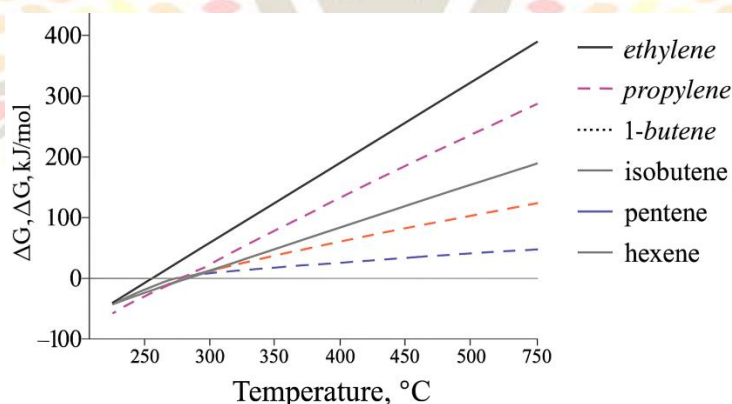


Figure 4. Effect of temperature on the thermodynamic stability of unsaturated ethylenic series hydrocarbons.

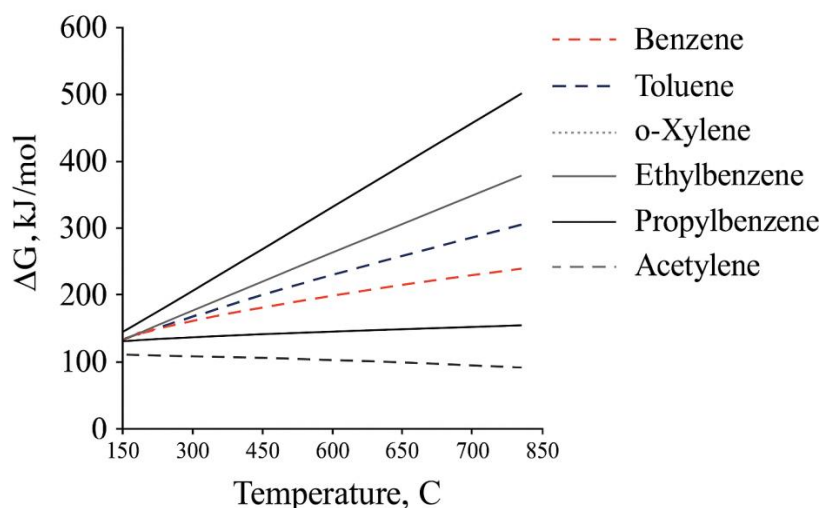


Figure 5. Effect of temperature on the thermodynamic stability of acetylene and aromatic hydrocarbons.

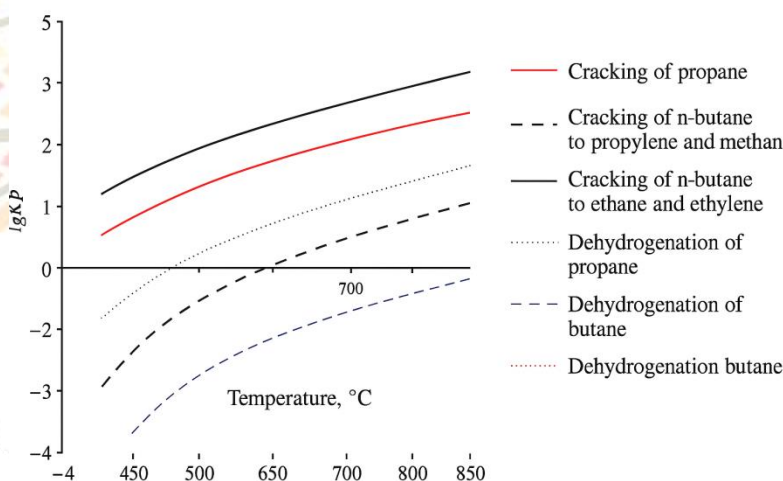


Figure 6. Temperature dependence of  $\lg K_p$  processes of transformation of low molecular weight saturated hydrocarbons.

Based on thermodynamic calculations, the equilibrium state and the change in the composition of products of low-molecular-weight saturated hydrocarbons such as propane and butane at different temperatures make it possible

to assess the mechanism and reaction conditions of very important processes.

#### Dehydrogenation of propane:

When a propane molecule is dehydrogenated, propylene ( $C_3H_6$ ) and hydrogen ( $H_2$ ) are formed as the main products. With increasing temperature, the reaction equilibrium shifts towards the products: at  $227^\circ C$ , the conversion is 0.12%, at  $627^\circ C$ , this value increases to 47.42%, and at  $827^\circ C$  to 86.99%. At the same time, the amount of  $H_2$  at equilibrium also increases from 18.49%  $\rightarrow$  46.52%, which clearly demonstrates the effect of temperature on an endothermic reaction.

### Dehydrogenation of butane.

Dehydrogenation of butane ( $C_4H_{10}$ ) produces butylene ( $C_4H_8$ ) and  $H_2$ . Butane achieves higher conversions at lower temperatures than propane:

Conversion at  $427^\circ C$  is  $\sim 13.7\%$ , at  $627^\circ C$   $\sim 48.0\%$ , and at  $727^\circ C$   $\sim 68.0\%$ .

This reaction is also endothermic, with the amount of  $H_2$  increasing with increasing temperature.

### Propane cracking reaction.

Thermal cracking of propane produces methane ( $CH_4$ ), ethane ( $C_2H_6$ ), ethylene ( $C_2H_4$ ) and other

low molecular weight fragments. At  $327^\circ C$ , the conversion is 53.3%, and at  $427^\circ C$ , the conversion is almost 100%. This indicates high reactivity and easy cleavage of C–C bonds. Cracking of butane (to propylene and methane) shows a 52.7% conversion of butane at  $227^\circ C$ , and almost 100% conversion at equilibrium at  $327^\circ C$ . The main products in this reaction are methane ( $CH_4$ ) and propylene ( $C_3H_6$ ).

### Cracking of butane to ethane and ethylene.

In this process, butane is converted to  $C_2H_6$  and  $C_2H_4$ : 27.96% conversion at  $327^\circ C$ ,  $\sim 52.83\%$  at  $427^\circ C$ , and  $\sim 100\%$  at  $527^\circ C$ . The main mechanism in this reaction is the cleavage of C–C bonds without the formation of  $H_2$ . Dehydrocarbonization reaction of butane (with C–C bond cleavage). In this reaction, carbon-carbon bonds are also cleaved along with butane dehydrogenation: 0.02% at  $227^\circ C$ , 23.11% at  $527^\circ C$ , and almost 100% at  $727^\circ C$ .

**Table 3. Equilibrium conversion of low molecular weight saturated hydrocarbons and equilibrium concentration of products.**

A lower molecular weight saturated hydrocarbon process	T, °C	Equilibrium of conversion of lower molecular weight saturated hydrocarbons, mol. (%)	The composition of the system in equilibrium, mol (%)								
			$C_3H_8$	$C_4H_{10}$	$CH_4$	$C_2H_6$	$C_2H_4$	$C_3H_8$	$C_4H_8$	$H_2$	
Dehydrog	227	0.1178	99.76	-	-	-	-	-	0.18	-	0.18



enation of propane	327	1.26	97.50	-	-	-	-	1.25	-	1.25
	427	6.82	87.24	-	-	-	-	6.38	-	6.38
	527	22.69	63.02	-	-	-	-	18.49	-	18.49
	627	47.42	35.66	-	-	-	-	32.17	-	32.17
	727	58.73	26.00	-	-	-	-	37.00	-	37.00
	827	86.99	6.96	-	-	-	-	46.52	-	46.52
Dehydrogenation of butane	227	0.2459	-	99,50	-	-	-	-	0,25	0,25
	327	2.61	-	94,90	-	-	-	-	2,55	2,55
	427	13.69	-	75,92	-	-	-	-	12,04	12,04
	527	40.09	-	42,76	-	-	-	-	28,62	28,62
	627	48.00	-	35,14	-	-	-	-	32,43	32,43
	727	68.02	-	19,04	-	-	-	-	40,48	40,48
	827	-	-	-	-	-	-	-	-	-
Propane cracking	127	1.59	96,86	-	1,57	-	1,57	-	-	-
	227	18.7	68,42	-	15,79	-	15,79	-	-	-
	327	53.32	30,44	-	34,78	-	34,78	-	-	-
	427	~100	0	-	-50	-	-50	-	-	-
Cracking of butane to propylene and methane	127	10.5	-	30,85	9,57	-	-	9,57	-	-
	227	52.70	-	30,98	34,51	-	-	34,5	-	-
	327	~100	-	0	-50	-	-	1	-	-
Cracking of butane to ethane and ethylene	127	0,3151	-	99,38	-	0,31	0,31	-50	-	-
	227	5,04	-	90,40	-	4,80	4,80	-	-	-
	327	27,96	-	56,30	-	21,85	21,85	-	-	-
	427	52,83	-	30,86	-	34,57	34,57	-	-	-
	527	~100	-	0	-	-50	-50	-	-	-
Processes involving the cleavage of the carbon-carbon bond of butane	227	0,020	-	99,94	-	-	0,04	-	-	0,02
	327	0,461	-	98,62	-	-	0,92	-	-	0,46
	427	4,338	-	88,03	-	-	7,98	-	-	3,99
	527	23,11	-	52,57	-	-	31,62	-	-	15,81
	627	85,67	-	5,47	-	-	63,02	-	-	31,51
	727	~100	-	0	-	-	66,7	-	-	33,3

This process is a deep cracking reaction that occurs at high temperatures, proceeds based on radical mechanisms and produces  $C_2H_4$ ,  $C_4H_8$  and  $H_2$  as the main products. Cracking reactions of  $C_3$ - $C_4$  saturated hydrocarbons in the range of 300-400°C give high conversions at equilibrium.

Dehydrogenation reactions reach equilibrium at 800-900°C. The composition of the products in different types of propane and butane reactions varies depending on the temperature, which is an important factor in optimising the process. The temperature regime should be selected depending

on the direction of the reaction (dehydrogenation, cracking, dehydro-cracking).

## CONCLUSION

In this study, methods for enhancing the sorption and catalytic activity of high-silica mesoporous zeolites (HSMZs) were developed through decationization in ammonium chloride solution and subsequent modification with various metal oxides. As a result, catalysts based on H-HSMZ modified with CuO, Li<sub>2</sub>O, La<sub>2</sub>O<sub>3</sub>, ZnO, Fe<sub>2</sub>O<sub>3</sub>, and BaO were synthesised and tested in the catalytic and thermal cracking of propane-butane fractions at high temperatures.

Experimental results revealed that, under high-temperature flow conditions, catalytic cracking exhibited higher conversion rates and better selectivity compared to thermal cracking. The catalytic performance was shown to depend significantly on both the type of metal oxide modifier and the catalyst preparation method (extrusion or tableting).

Structural analysis by infrared (IR) spectroscopy and X-ray diffraction (XRD) confirmed the high crystallinity of the zeolite samples and the preservation of the aluminosilicate framework structure. Thermodynamic analysis allowed for the assessment of equilibrium conditions, product distributions, and temperature-dependent stabilities of various reaction pathways involving propane and butane.

Based on the thermodynamic evaluation, an optimal temperature range of 650–800 °C was

recommended for achieving high selectivity toward the production of unsaturated hydrocarbons such as ethylene and propylene. Overall, the developed HSMZ-based catalysts and the defined operating conditions offer significant potential for improving the efficiency of converting propane-butane fractions into valuable light olefins.

## REFERENCES

1. Swesi, Y.; Kerleau, P.; Pitault, I.; Heurtaux, F.; Ronze, D. Purification of hydrogen from hydrocarbons by adsorption for vehicle applications. *Sep. Purif. Technol.* 2007, 56, 25–37.
2. Shelepova, E.V.; Vedyagin, A.A.; Mishakov, I.V.; Noskov, A.S. Simulation of hydrogen and propylene coproduction in catalytic membrane reactor. *Int. J. Hydrog. Energy* 2015, 40, 3592–3598.
3. Newborough, M.; Cooley, G. Developments in the global hydrogen market: The spectrum of hydrogen colours. *Fuel Cells Bull.* 2020, 16–22.
4. Al-Fatesh, A.S.; Fakeeha, A.H.; Khan, W.U.; Ibrahim, A.A.; He, S.; Seshan, K. Production of hydrogen by catalytic methane decomposition over alumina supported mono-, bi- and tri-metallic catalysts. *Int. J. Hydrog. Energy* 2016, 41, 22932–22940
5. Chesnokov, V.V.; Chichkan, A.S. Production of hydrogen by methane catalytic decomposition over Ni–Cu–Fe/Al<sub>2</sub>O<sub>3</sub> catalyst. *Int. J. Hydrog. Energy* 2009, 34, 2979–2985.
6. Silva, R.R.C.M.; Oliveira, H.A.; Guarino, A.C.P.F.; Toledo, B.B.; Moura, M.B.T.; Oliveira, B.T.M.;

- Passos, F.B. Effect of support on methane decomposition for hydrogen production over cobalt catalysts. *Int. J. Hydrog. Energy* 2016,41, 6763–6772.
7. Syed Muhammad, A.F.; Awad, A.; Saidur, R.; Masiran, N.; Salam, A.; Abdullah, B. Recent advances in cleaner hydrogen productions via thermo-catalytic decomposition of methane: Admixture with hydrocarbon. *Int. J. Hydrog. Energy* 2018,43, 18713–18734
8. Jian, X.; Jiang, M.; Zhou, Z.; Zeng, Q.; Lu, J.; Wang, D.; Zhu, J.; Gou, J.; Wang, Y.; Hui, D.; et al. Gas-Induced Formation of Cu Nanoparticles as Catalyst for High-Purity Straight and Helical Carbon Nanofibers. *ACS Nano* 2012,6, 8611–8619.
9. Simon, A.; Seyring, M.; Kämnitz, S.; Richter, H.; Voigt, I.; Rettenmayr, M.; Ritter, U. Carbon nanotubes and carbon nanofibers fabricated on tubular porous Al<sub>2</sub>O<sub>3</sub> substrates. *Carbon* 2015, 90, 25–33.
10. Bayat, N.; Rezaei, M.; Meshkani, F. Methane decomposition over Ni-Fe/Al<sub>2</sub>O<sub>3</sub> catalysts for production of CO<sub>x</sub>-free hydrogen and carbon nanofiber. *Int. J. Hydrog. Energy* 2016,41, 1574–1584.
11. Fakeeha, A.H.; Ibrahim, A.A.; Khan, W.U.; Seshan, K.; Al Otaibi, R.L.; Al-Fatesh, A.S. Hydrogen production via catalytic methane decomposition over alumina-supported iron catalyst. *Arab. J. Chem.* 2018,11, 405–414.
12. Shen, Y.; Lua, A.C. Synthesis of Ni and Ni-Cu supported on carbon nanotubes for hydrogen and carbon production by catalytic decomposition of methane. *Appl. Catal. B Environ.* 2015, 164, 61–69.
13. Ping, D.; Wang, C.; Dong, X.; Dong, Y. Co-production of hydrogen and carbon nanotubes on nickel foam via methane catalytic decomposition. *Appl. Surf. Sci.* 2016, 369, 299–307.
14. Karaismail oglu, M.; Figen, H.E.; Baykara, S.Z. Hydrogen production by catalytic methane decomposition over yttria-doped nickel-based catalysts. *Int. J. Hydrog. Energy* 2019,44, 9922–9929
15. Berndt, F.M.; Perez-Lopez, O.W. Catalytic decomposition of methane over Ni/SiO<sub>2</sub>: Influence of Cu addition. *React. Kinet. Mech. Catal.* 2016,120, 181–193.